

# Elastic Critical Load Characterization of Ellipsoidal Shells of Revolution: Design Study and Generalized Shell Parameters

VVNL Sravanthi<sup>1</sup>, Prof. V. Diwakar Reddy<sup>2</sup>, Prof. G. Krishnaiah<sup>3</sup>

<sup>1, 2, 3</sup> Dept. Of Mechanical Engg, Sri Venkateswara University College of Engg, Tirupati

**Abstract:** Shells are used for multiple load bearing applications due to their attractive property of high stiffness to weight ratio. Various studies were reported in literature on buckling, free vibration and elastic-plastic transition of hemispherical shells. Few studies dealt with ellipsoidal shells subjected to internal/external pressure. In this paper, we study the elastic critical load characteristics of ellipsoidal shells of revolution subject to compression, targeting a load sensing application. A validated finite element model is built to perform a careful unified study of multiple design configurations and new generalised shell parameters are proposed which represent both hemispherical and elliptical configurations. This helps the designers explore a larger design space in a unified framework and arrive at an optimum configuration.

**Keywords:** Shells, Elastic critical load, Ellipsoidal shells of revolution, Finite Element Analysis

## I. INTRODUCTION

Shells subjected to rigid plate compression have been studied extensively in the literature. Many of the studies analysed the hemispherical cross-section subjected to loads in both elastic and plastic regimes. Over the years, methods of varying fidelity have been used to detail the load-deformation behaviour of these shells under compression. In particular, buckling characteristics were reported for different thickness ratios, height ratios and material properties. A brief overview of the prior literature is detailed below along with motivation for the present study.

With regards to hemispherical shells, Reissner[1] investigated the shell-plate contact problem and provided expressions for direct and bending stresses for shallow shells with  $h/R < 4$ . Naghdi[2] later extended Reissner's study to include the effect of shear strains. Kalnins[3] devised a multi-segment method for nonlinear analysis of elastic shells. Updike et al[4] investigated the load behavior of an compressed elastic shell, coming up with an analytical formulation for elastic load-deflection and also buckling phenomena wherein the shell deforms with an axisymmetric dimple at the center. Subsequent studies by Shwarz[5] and Kitching[6] focused on load-interference behavior as a function of shell thickness and radius. Interestingly, they were looking at contrasting shell applications, one concerning cornea and other collision of vehicles. Gupta et al[7] focused on buckling of hemispherical shells across a range of thickness ratios ( $R/t : 15$  to  $240$ ) and showed good agreement between experimental and theoretical results. Another interesting shell load application to ping pong ball was studied by Pauchard et al[8]. Shariati et al[9] performed experimental and numerical study of buckling behavior of steel shells with flat tops under various loadings. The study of Longqiu Li et al[10] provides a pointer in using FE model to derive useful information on onset of plastic yielding but is limited to the treatment of hemi-spherical shells. Other recent studies on deformation behavior of hemispherical shells are captured in references [11] and [12].

In the context of ellipsoidal shells of revolution, majority of published articles focused on either free vibration or buckling behavior. Ref [13] provides a comprehensive review of literature on ellipsoidal shells, the analytical theory development and their application space. It can be seen that typical example applications of ellipsoidal shells dealt in literature are heads of pressure vessels or domes of buildings/structures where internal pressure or uniform external loading is the loading scenario. Here we will analyze and quantify the elastic critical loading capacity of ellipsoidal shell for load sensing applications. The study attempts to unify the behavior of hemispherical and ellipsoidal shells under a common framework. Such an approach has the advantage of analyzing the full spectrum of design space and offers a unique perspective of how conventional shells fit in the load-deformation behavior of generic elliptical shells. Several DoE studies were performed to depict the variation of elastic critical load and deformation. A validated finite element model is used to analyze the stress limits within the thickness of the shells as a function of geometry. Also, new generic non-dimensional shell parameters valid for both elliptic and circular cross-sections are proposed which can be applied during the design phase to choose the optimum shell parameters per desired load application. Next section shows details of the load

device setup. To enable such an application of shell geometries, it is imperative to demonstrate high elastic load bearing capacity with a compact configuration, which forms the subject of present study.

## II. LOAD DEVICE SCHEMATIC, DESIGN PARAMETERS AND MODEL SETUP

Fig.1 show the loading device setup, which is to be designed with maximum elastic load bearing capability. The deformation of the device will be transmitted to a piezo device to calibrate the input load. They are placed at multiple locations along the load device to average out the non-uniformities and provide a robust load indication.

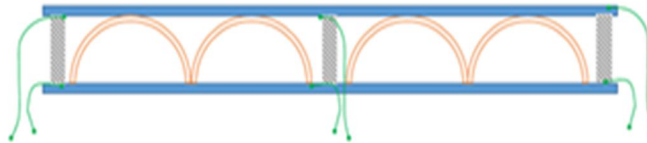


Fig.1 Load device with multiple shell arrangement. Grey blocks are piezo transducers

The layout of multiple shells can be chosen based on the application (space and desired load capability). Some of the arrangements are shown below in Fig.2 for reference.

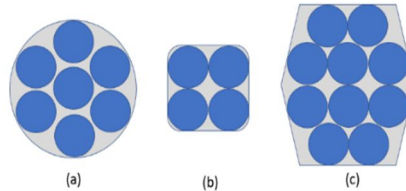


Fig. 2 Possible shell arrangements in top view (circular, square, hexagonal)

### A. Shell Parameters & Design Space

In order to facilitate the study of wider design space and establish generalized conclusions, an ellipsoidal shell of revolution is constructed according to Eq(1). The consideration of generic elliptic shape gives insights on extensibility of hemi-spherical shell results to other aspect ratios. Equation of ellipsoidal shell of revolution:

$$\frac{x^2}{a^2} + \frac{y^2}{b^2} = 1 \tag{1}$$

b – semi minor axis of the ellipse (also used interchangeably with shell height and baseline solid sphere radius)

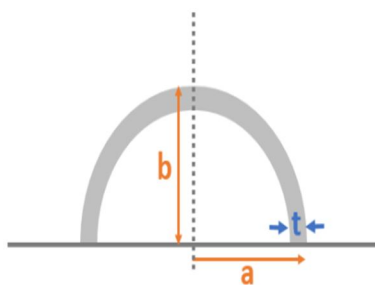


Fig. 3 Shell cross-section design parameters

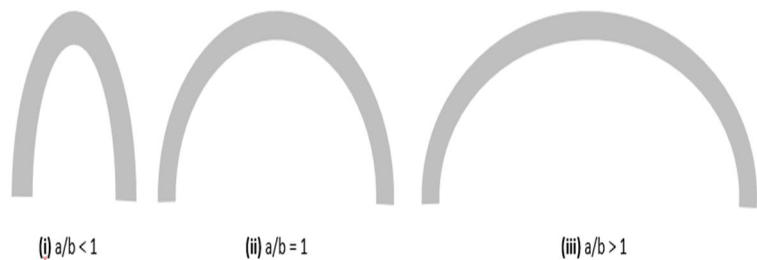


Fig. 4 Elliptic shell cross-sections (prolate, circular, oblate)

As shown in Fig 4, geometries with  $a/b < 1$  are referred to as prolate which have high curvature near contact zone and the converse happens for  $a/b > 1$  which are referred to as oblate configurations. For the parametric study,  $a/b = 1$  geometries are considered since the objective is to quantify the increase in load capacity as the contact curvature flattens out for increasing  $a/b$ . The semi-minor axis (b) is equal to the height of the shell. Following table presents the different parameter combinations analysed in this work. For each elliptical shell shape ( $a/b$ ), a range of thickness variation is considered to capture optimum value at which load capacity attains a maximum. As shown in Table 1, a total of 75 finite element simulations are performed. The thickness ratios ( $t/R$ ) also cover broader range compared to values reported in literature.

Parameter	Min Value	Max Value	# Steps
a/b	1.0	1.5	3
t/b	0.02	0.5	25

Table 1. Design Variable variations analysed in the study

The material property contribution, which influences the load capacity is inherently accounted for through the use of spherical shell design parameter ( $\lambda$ ) as will be shown later.

**B. Finite Element Model**

An axi-symmetric finite model is built to perform the design of experiments in Ansys as shown in Fig 5. It consists of shell model which can be varied in shape depending on choice of a/b & t/b.

On the symmetry end, model is constrained in horizontal direction and model is fixed in all directions on the bottom face of the shell. ANSYS axi-symmetric shell element PLANE183 is used to model shell & rigid plate. The top plate is made rigid by imposing young’s modulus of 1000 times the shell material. Displacement is applied on the top rigid plate and is gradually applied in 100 steps for accurately capturing the non-linear contact and elastic-plastic transition. For contact modelling, all the top faces of the shell are selected and connected with the nodes on the bottom face of the rigid plate. The young’s modulus of the shell material is taken as 180MPa and poisson’s ratio as 0.31. The typical mesh count of the model is ~35000. Meshes of different resolution were used in the shell, with finer count of ~100 elements per shell thickness near the contact zone gradually coarsening to ~10 elements per shell thickness at the fixity. Von-mises criterion is used to identify the onset of plasticity. The zoomed portion of the mesh near the contact region is also shown in Fig 5.

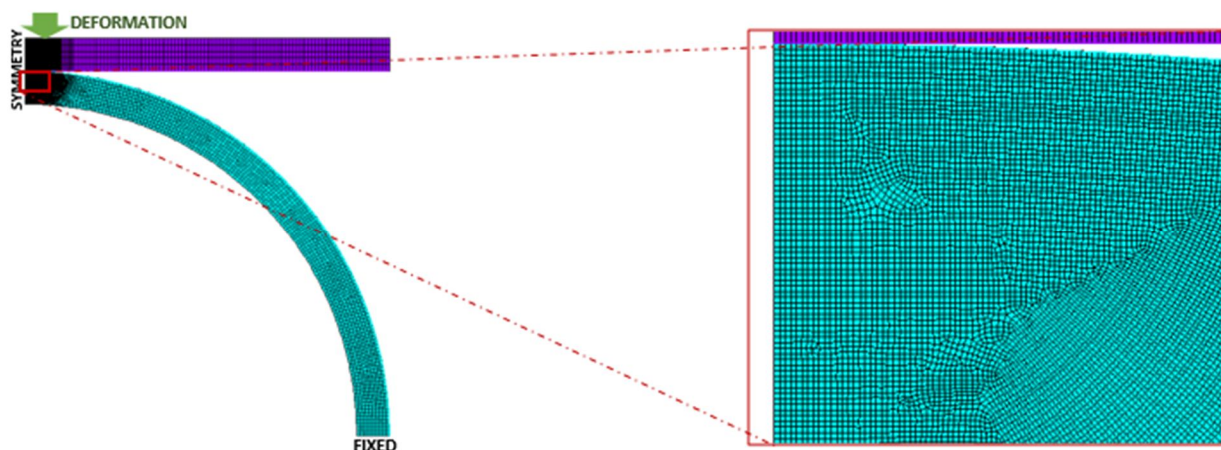


Fig. 5 Finite Element Model of shell along with zoomed portion of the mesh near contact zone

**III.RESULTS AND DISCUSSION**

The results are arranged in different sections to study various aspects of load capacity, deformation, unified shell parameters and weight of the load device under consideration.

**A. Elastic Critical Load Capacity**

The elastic critical load is the maximum load the structure can take without deforming into plastic zone. This is important as it limits the maximum load that can be sensed by the device while ensuring reusability. The variation of critical load with elliptic ratio(a/b) and thickness ratio(t/b) variation are depicted in Fig 6. They are plotted against the spherical shell parameter ( $\lambda$ ) on X-axis. On Y-axis, the elastic critical load of the shell is normalized with the corresponding load for solid sphere defined as follows.

$$\text{Critical load for solid sphere: } P_{crit-sphere} = \frac{\pi^3}{6} C_v^3 Y \left( R(1 - \nu^2) \frac{Y}{E} \right)^2 \tag{2}$$

$$\text{Increase in elastic load capacity (plotted on Y-axis): } \gamma = \frac{P_{crit}}{P_{crit-sphere}} \tag{3}$$

Shell Parameter (plotted on X-axis):  $\lambda = \log\left(\frac{t}{R}\left(\frac{E}{Y}\right)^{0.886}\right)$  (4)

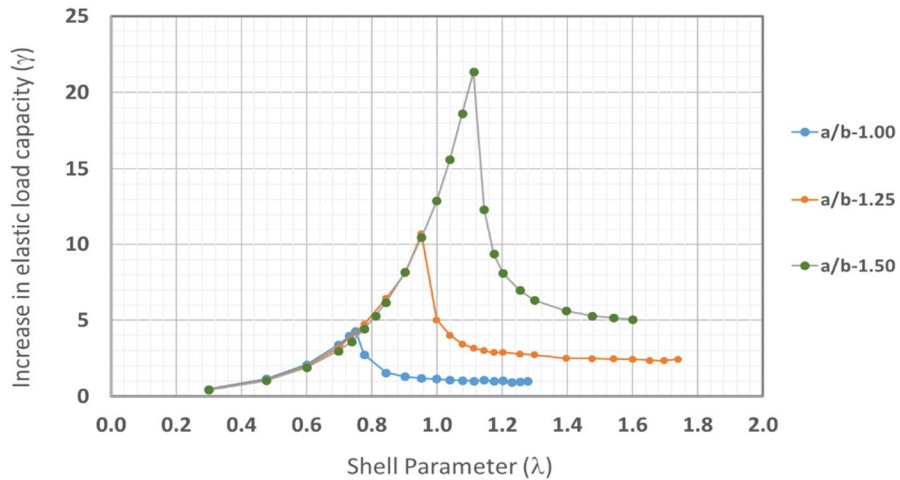


Fig. 6 Variation of Elastic critical load with ellipse ratio and thickness ratio

1) The following key Observations Can be Made From The Critical Load Capacity Chart.

- a) The maximum load capacity for hemispherical shell (a/b of 1) is ~4 at  $\lambda$  of ~0.75 which matches the results reported in Ref[10], thus validating the finite element model.
- b) As the ellipse ratio increase, there is a significant increase in maximum elastic load capacity of the shell rising from a max value of 4 for a/b-1 to >20 for a/b-1.5.
- c) At low values of  $\lambda$ , all curves coincide which indicates no benefit in load capacity.
- d) The thickness value at which the peak load occurs shifts significantly to the right i.e. towards higher  $\lambda$  values. Since the shell parameter has both material properties and thickness ratio, this can be interpreted in 2 different ways. If material is same, thickness ratio increases towards the right and if the thickness ratio is fixed, it amounts to higher E/Y ratio.
- e) All curves show sharp peaks after which sudden transition occurs from high load capacity to a downward trend.

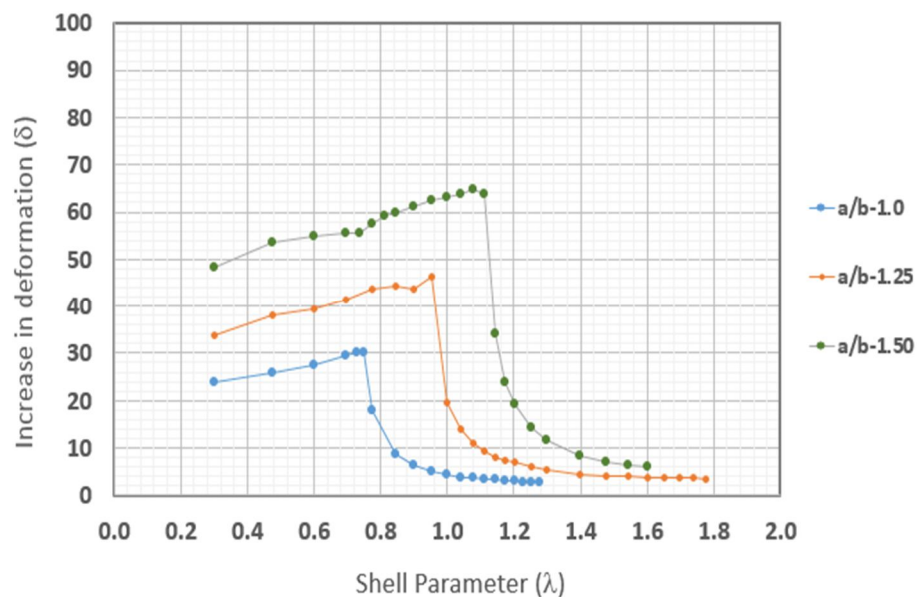


Fig. 7 Variation of deformation with ellipse ratio and thickness ratio

The behaviour of shell deformation is shown in Fig 7. The shell parameter on X-axis is same as before while the deformation increase on Y-axis is characterized as below.

$$\text{Critical deformation for solid sphere: } \omega_{crit-sphere} = \frac{\pi}{2} C_v R (1 - \nu^2) \left(\frac{Y}{E}\right)^2 \tag{5}$$

The deformation also increases for the higher ellipse ratios ( $a/b > 1$ ), which would be helpful in load calibration/measurement. The steep drop in deformation beyond a certain thickness ratio, coincides with the peak load capacity of Fig 6. So, for the same material ( $E/Y$ ), this is the point where the shell starts to become stiff due to increase in thickness ratio.

**B. Generalized Shell Parameter (Hemispherical and Elliptic Shells)**

Careful observation of Fig 6 reveals that there might exist a relation between the increase in load capacity as the ellipse ratio increases. Such a relation would be very valuable as it generalizes the analyses of shells irrespective of whether it is hemispherical or elliptical shape. The load capacity varies as 4<sup>th</sup> power of ellipse ratio (Fig 8) and the shell parameter varies linearly with ellipse ratio resulting in the relations shown by Eq(8) and Eq(9). With this, all the three graphs of Fig 6 come together using the new parameters as in Fig 9.

$$\text{New generalized parameter for load capacity ratio: } \gamma^* = \gamma \left(\frac{b}{a}\right)^4 \tag{8}$$

$$\text{New generalized shell parameter: } \lambda^* = \lambda \left(\frac{b}{a}\right) \tag{9}$$

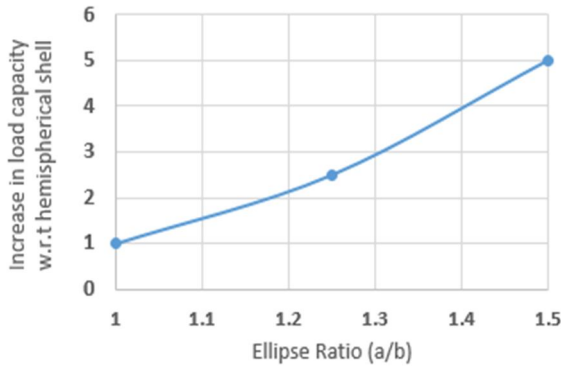


Fig 8 Load capacity increase vs Ellipse Ratio

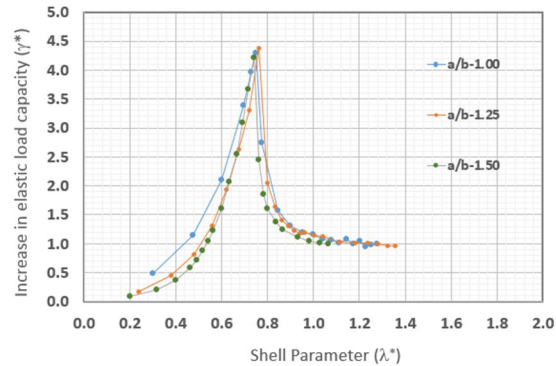


Fig 9 : Unified load chart for hemispherical and ellipsoidal shells

**C. Increase in load vis-à-vis Weight**

In Fig 6, we have seen that load increase for high ellipse ratios is achieved at higher thickness ratios implying an increase in weight. For a compact load device, it is imperative that load capacity increase should be offset by the weight ratio. In this section, we demonstrate the effectiveness of going to higher ellipse ratios, for which Fig 6 is recast with X-axis as weight ratio compared to solid sphere. From this, one can compute the ratio of ellipse shell weight to hemispherical shell weight. Analysing the shapes, it is easy to show that weight ratio is given by Eq 10.

$$\text{Weight Ratio } \sigma = \frac{a}{b} - \left(\frac{a}{b} - \frac{t}{b}\right) \left(1 - \frac{t}{b}\right) \tag{10}$$

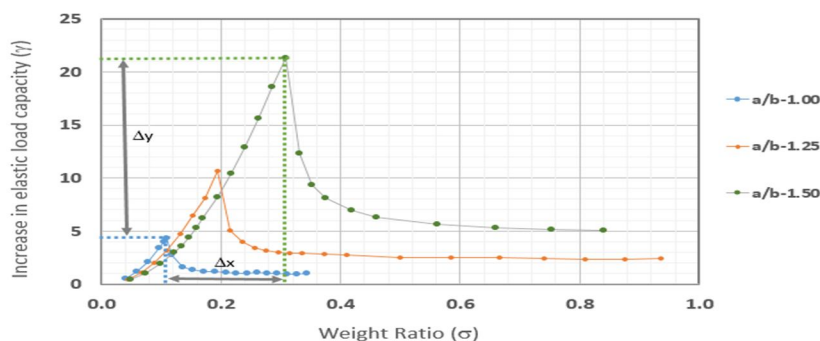


Fig 10 Tradeoff chart between critical load increase and weight increase

It can be seen that the increase in load capacity (~5X) is higher than increase in shell weight (~3X) and hence the elliptical configuration would be a beneficial design modification to the load device.

#### IV. CONCLUSIONS

A unified study of hemispherical and ellipsoidal shells of revolutions has been carried out to assess the elastic critical load capacity and also to develop unified shell parameters applicable to both configurations. The intended load sensing application has been detailed to provide the context and also the objective to increase the critical load beyond what the hemispherical shell offers. Through a validated finite element model, the increase in critical load has been quantified to be beyond a factor of 5 compared to hemispherical shell. Careful observation has led to definition of new generalized shell parameters which would collapse all the graphs through the inclusion of ellipse ratio. Also, weight tradeoff study is performed which demonstrates that load increase overcomes the weight increase associated with high ellipse ratios and shell thickness.

#### V. ACKNOWLEDGMENTS

We sincerely acknowledge the support of Sri Venkateswara University College of Engg for providing an opportunity to study the behaviour of shells for load sensing applications.

#### VI. NOMENCLATURE

a = Semi-major axis of ellipse

b = Semi-minor axis of ellipse (also interchangeably used with shell height and radius of baseline solid sphere)

R = Radius of the baseline solid sphere

t = Shell thickness

E = Young's Modulus of the shell material

Y = Yield Strength

$\nu$  = Poisson's Ratio ;  $C_\nu = 1.234 + 1.256\nu$

#### REFERENCES

- [1] Reissner, E., 1947, "Stresses and Small Displacements of Shallow Spherical Shells," J. Math. Phys., 25\_3\_, pp. 279-300.
- [2] Naghdi, P., 1956, "Note on the Equation for Shallow Spherical Shells," Q. Appl. Math., 14, pp. 369-380.
- [3] Kalnins, A., Lestingi., 1967, "On Nonlinear Analysis of Elastic Shells of Revolution," J. Applied Mechanics., pp. 59-64.
- [4] Updike, D.P., Kalnins, A., 1970, "Axisymmetric Behaviour of an Elastic Shell compressed between Rigid Plates," J. Applied Mechanics., pp. 635-640.
- [5] Schwartz, N. J., Mackay, R. S., and Sackman, J. L., 1966, "A Theoretical and Experimental Study of the Mechanical Behavior of the Cornea With Application to the Measurement of Intraocular Pressure," Bull. Math. Biophys., 28\_4\_, pp. 585-643.
- [6] Kitching, R., Houlston, R., and Johnson, W., 1975, "A Theoretical and Experimental Study of Hemispherical Shells Subjected to Axial Loads Between Flat Plates," Int. J. Mech. Sci., 17, pp. 693-703.
- [7] Gupta, P. K., and Gupta, N. K., 2006, "An Experimental and Computational Study of the Crushing of Metallic Hemispherical Shells Between Two Rigid Flat Plates," J. Strain Anal. Eng. Des., 41\_6\_, pp. 453-466.
- [8] Pauchard, L., and Rica, S., 1998, "Contact and Compression of Elastic Spherical Shell: The Physics of a 'Ping Pong' Ball," Philos. Mag. B, 78, pp. 225-233.
- [9] Shariati, M., Allahbakhsh, H. R., 2010, "Numerical and experimental investigations on the buckling of steel semi-spherical shells under various loadings," Thin-Walled Structures, 48, pp. 620-628.
- [10] Longqiu Li, et al., 2011, "The Onset of Plastic Yielding in a Spherical Shell Compressed by a Rigid Flat," J. Applied Mechanics., 78, pp. 1-7
- [11] Shahin Nayyeri Amiri, Hayder A. Rasheed, 2012, Plastic buckling of moderately thick hemispherical shells subjected to concentrated load on top, International Journal of Engineering Science, Volume 50, Issue 1, January 2012, Pages 151-165
- [12] YANG et al, Peripheral Deformation and Buckling of Stainless Steel Hemispherical Shells Compressed by a Flat Plate. Lat. Am. j. solids struct. [online]. 2016, vol.13, n.2, pp.257-271. ISSN 1679-7817
- [13] S. N. Krivoshapko, Research on General and Axisymmetric ellipsoidal shells used as Domes, Pressure Vessels and Tanks , J. Applied Mechanics, pp 336-355, Vol 60, November 2007.